Cell-to-Cell Information at a Feedback-Induced Bifurcation Point

Amir Erez[ORCID],[1] Tommy A. Byrd,[2] Michael Vennettilli,[2] and Andrew Mugler[ORCID][2,*]

[1]*Department of Molecular Biology, Princeton University, Princeton, New Jersey 08544, USA*
[2]*Department of Physics and Astronomy, Purdue University, West Lafayette, Indiana 47907, USA*

A ubiquitous way that cells share information is by exchanging molecules. Yet, the fundamental ways that this information exchange is influenced by intracellular dynamics remain unclear. Here we use information theory to investigate a simple model of two interacting cells with internal feedback. We show that cell-to-cell molecule exchange induces a collective two-cell critical point and that the mutual information between the cells peaks at this critical point. Information can remain large far from the critical point on a manifold of cellular states but scales logarithmically with the correlation time of the system, resulting in an information-correlation time trade-off. This trade-off is strictly imposed, suggesting the correlation time as a proxy for the mutual information.

Cells sense and respond to their environment, transforming chemical cues into the modification of signaling molecules, the expression of genes, and the production of proteins. Such signaling networks are often complex, involving, among other features, multiple feedback loops. Yet, the underlying purpose of these networks is to sense and transmit information robustly. For example, in the context of immune response, the complex topology of signaling cascades in T cells can be such that perturbing a cascade before or after a feedback loop results in dichotomous response [1]. However, coarse graining the signaling cascade, one can define a basic unimodal-bimodal system, agnostic of biological details, which singles out a particular "readout" molecule while integrating out all others. Such coarse graining of the network results in an effective feedback term, which reduces the dynamics to a universal form near a bifurcation point [2–4]. As a result, one can apply critical scaling to these universal dynamics, modified by their nonequilibrium nature [5].

Though powerful, such analysis of intracellular dynamics alone treats cells in isolation, equivalent to a very dilute suspension. This ignores the role of cell-to-cell interactions, communicated by means of molecule exchange. Such communication in its simplest form involves only two cells, either similar or different, which produce, degrade, and exchange a molecule. Interaction between two cells is an important biological process, e.g., the immunological synapse [6,7]. By modeling molecule exchange between two cells, with each cell a generic sense-and-secrete apparatus, one can study the fundamentals of cell-to-cell information. Investigating the information exchange between two cells in this simple framework is the focus of this work.

Model.—Within each cell, biochemical reactions in a complex signaling cascade have the net effect of producing and degrading a molecular species of interest. We specialize to dynamics that can yield either a unimodal or a bimodal molecule number distribution in steady state. Near such a bifurcation point, as was previously shown [3], the precise form of the coarse-grained feedback is irrelevant. For convenience we choose to parameterize it using Schlögl's second model [8–15], a well-studied set of reactions that minimally encodes feedback. Specifically, as illustrated in Fig. 1(a), in the first (second) cell, species X (Y) can be produced spontaneously from bath species at rate k_1^+ (q_1^+), and can be produced nonlinearly at rate k_2^+ (q_2^+) via a trimolecular reaction involving two existing X (Y) species and a bath species. Species X (Y) can be degraded linearly with molecule number at a rate k_1^- (q_1^-), or in a reaction involving three existing X (Y) molecules at rate k_2^- (q_2^-). In addition to the internal reactions, X (Y) can be exchanged from the neighboring cell at rate γ_{xy} (γ_{yx}). Physically, this can be through a gap junction or through diffusion. Individually, in the absence of exchange ($\gamma_{xy} = \gamma_{yx} = 0$), each of the two constituent cells' molecule number distribution can be either unimodal or bimodal, depending on parameters. If exchange is switched on, ($\gamma_{xy}, \gamma_{yx} > 0$), the system converges to a collective two-cell state, with the joint distribution unfactorizable in general, $P(X, Y) \neq P_X(X)P_Y(Y)$.

Thermodynamic parameters.—Building upon previous work [3,5], we construct a mapping from Schlögl parameters to Ising-like parameters. Without exchange, the deterministic dynamics corresponding to the reactions in the left cell in Fig. 1(a) are $dx/dt = k_1^+ - k_1^- x + k_2^+ x^2 - k_2^- x^3$, where we have neglected the small shifts of -1 and -2 for large x. Defining the order parameter $m = (x - n_c)/n_c$, we choose n_c to eliminate the term quadratic in m, putting the dynamics in the Landau form [3]

$$\frac{dm}{d\tau} = h - \theta m - \frac{m^3}{3}, \qquad (1)$$

where we have defined $n_c = k_2^+/3k_2^-$, $\tau = (k_2^+)^2 t/3k_2^-$, $\theta = 3k_1^- k_2^-/(k_2^+)^2 - 1$, and $h = 9k_1^+(k_2^-)^2/(k_2^+)^3 - 3k_1^- k_2^-/(k_2^+)^2 + 2/3$.

The number of molecules in the system is controlled by n_c. In fact, n_c controls all scaling properties of the single-cell system, acting as a finite system size of the equivalent critical Ising system [3]. Roughly, in our system, n_c is the value of X or Y at the center of the flat part of the critical distribution ($\theta = 0$) in Fig. 1(b). At small n_c, therefore smaller molecule numbers, small corrections to this mapping can be derived by expanding the known stochastic steady-state distribution around its maximum instead of relying on the deterministic dynamics (see the Supplemental Material [16]). We use the corrected mapping in all simulations in this work.

In steady state, $dm/d\tau = 0$. We can thus interpret m as an order parameter for the single-cell system, $\theta \equiv (T - T_c)/T_c$ as a reduced "temperature," and h as a dimensionless field. Analogous to the Ising model, when $h = 0$ in the single-cell system, $\theta > 0$ corresponds to a unimodal steady-state distribution, and $\theta < 0$ to a bimodal distribution. Similarly, tuning h biases the distribution to high or low molecule count. The stochastic steady state of a single cell at m, θ, $h = 0$ was previously shown to exhibit many properties of equilibrium critical points [3]. Applying the same mapping to two coupled cells (with $k \to q$ for Y) results in the Landau form,

$$\frac{dm_X}{d\tau} = h_X - \theta_X m_X - \frac{m_X^3}{3} + g_{XY} m_Y - g_{YX} m_X, \qquad (2)$$

$$\frac{dm_Y}{d\tau} = h_Y - \theta_Y m_Y - \frac{m_Y^3}{3} + g_{YX} m_X - g_{XY} m_Y, \qquad (3)$$

where $g_{XY} = 3\gamma_{xy} k_2^-/(k_2^+)^2$ and $g_{YX} = 3\gamma_{yx} q_2^-/(q_2^+)^2$ parametrize the exchange terms between cells.

The joint distribution $P(X, Y)$ for *identical* cells is shown in Fig. 1(b): with identical dimensionless fields ($h_X = h_Y = 0$), internal reaction rates ($k_{1,2}^\pm = q_{1,2}^\pm$), molecular diffusion strengths ($g_{XY} = g_{YX} = g$), reduced temperatures ($\theta_X = \theta_Y = \theta$), and system size ($n_{c,X} = n_{c,Y}$). In the top row there is no molecular exchange between cells ($g = 0$), and each cell is governed solely by its internal dynamics, $P(X, Y) = P_X(X) P_Y(Y)$. Negative θ yields a *polarized*, bimodal marginal distribution for each cell, $P_X(X)$ and $P_Y(Y)$. Stochastic fluctuations induce switching between states in each cell individually, resulting in four modes in $P(X, Y)$. When $\theta = 0$, each cell sits at its own critical point, resulting in broad and flat marginal distributions, with the joint distribution square shaped. When $\theta > 0$, each cell is *centralized*, yielding a unimodal marginal distribution about n_c, with the joint distribution also centralized. In the bottom row of Fig. 1(b), the effect of
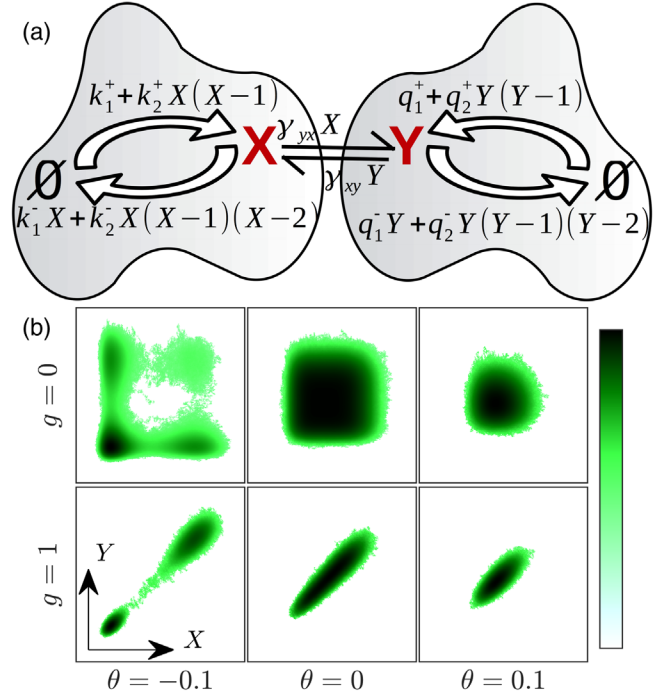

FIG. 1. Model and simulated distributions. (a) Two-cell Schlögl dynamics with an exchange term γ. (b) Examples of the joint distribution $P(X, Y)$ from Gillespie simulations with $h = 0$ for $g = 0$ (top) and $g = 1$ (bottom). Color map corresponds to $\log P$.

molecule exchange ($g = 1$) is evident. When $\theta < 0$, each cell is polarized, and can again access two distinct internal states, but their joint distribution reveals that the cells switch states in concert. When $\theta = 0$, each cell can access a broad range of molecule numbers, but exchange induces the cells to have nearly equal molecule number at all times. This effect is also seen when $\theta > 0$, in a smaller, centralized range of accessible molecule numbers.

Having established that two communicating cells undergo a bifurcation in their collective dynamics at $\theta = 0$, we ask: what are the properties of the two-cell bifurcation point? One can read out the mean-field critical exponents $\beta = 1/2$, $\gamma = 1$, $\delta = 3$ directly from the two-cell Landau form. For the exponent α, the single-cell system shows a *minimum* of its heat capacity C_v at $\theta = 0$ [3], with peak depth depending on the "system size" n_c. Similarly, for the two-cell system, we calculate C_v directly from the empirical $P(X, Y)$ using $C_v = (1 + \theta)(\partial S/\partial \theta)$ and the Shannon entropy $S = -\sum_{X,Y} P(X, Y) \ln P(X, Y)$. We plot $C_v(\theta, n_c)$ for a range of n_c values in Fig. 2(a), confirming a minimum of C_v at $\theta = 0$, with $C_v(\theta = 0) \sim n_c^{1/2}$ (inset). Therefore, at steady state, the two communicating cells near their bifurcation point are in the same static mean-field universality class as the single-cell system.

When considering the stochastic dynamical system at its bifurcation point in steady state, or its representation as the critical point of two coupled Ising models, an important timescale emerges: the correlation time, τ. The correlation
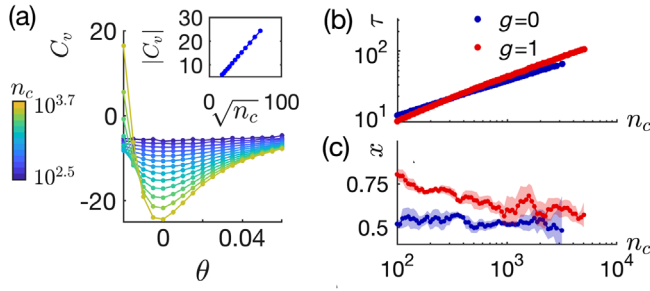
FIG. 2. Scaling of heat capacity and correlation time. (a) The heat capacity C_v reaches a minimum at $\theta = 0$; Inset—the depth of $C_v(\theta = 0)$ scales as $\sqrt{n_c}$. (b) Correlation time τ at $\theta = 0$, dependence on n_c, blue: $g = 0$ (no exchange); red: $g = 1$. (c) Estimate of the local slope $x = d\ln\tau/d\ln n_c$ from the data in (b), shaded area: 95% confidence interval.

FIG. 3. Shannon mutual information for identical cells. (a) Shannon mutual information I, for θ, $h = 0$; colors correspond to increasing n_c values from $10^{2.5}$ (blue) to $10^{3.7}$. Dashed horizontal marks $\theta = 0$. (b) $I(n_c; \theta = 0)$ for different values of $g \in \{10^{-1}, 10^{-0.5}, 10^0, 10^{0.5}\}$. Dashed black—showing that $I(n_c) = \text{const} + \ln n_c^{1/4}$ (c) Heat map showing $I(\theta, h)$ dependence on both θ and h with $g = 1$ and $n_c = 3000$.

time controls the response of the system to both sudden and gradual changes, a common and important biological scenario, e.g., in the dynamics of response to small-molecule drugs [5]. Figure 2(b) shows the dependence of correlation time, τ on the system size n_c, computed from Gillespie simulations with $\theta = h = 0$ using the method of batch means [17]. The two curves represent a simulation with exchange (red, $g = 1$) and without it (blue, $g = 0$). To find x in $\tau \sim n_c^x$, in Fig. 2(c) we plot the local slope, $x = d\ln\tau/d\ln n_c$ from Fig. 2(b). Without exchange, van Kampen's "system size" expansion shows that $x = 1/2$ [3,18], and this value is confirmed by the blue curve in Fig. 2(c). With exchange, x is greater than $1/2$ with x tending towards $1/2$ as n_c increases.

In the language of our Ising-like parameters (h, θ), what values result in the highest cell-to-cell information? We quantify information by means of the Shannon mutual information, I, shown in Fig. 3(a) for identical cells, with $h = 0$. Each curve represents a different system size, n_c. As n_c increases, I peaks closer to the critical point, $\theta = 0$. When $\theta < 0$, as shown in Fig. 1(b), the polarized bimodal regime inhibits stochastic switching, reducing information exchange. Conversely, when $\theta > 0$, noise dominates communication, suppressing I. Moreover, Fig. 3(b) shows that $I(n_c, g, \theta = 0) \sim \ln n_c^{1/4}$, to be contrasted with $\tau \sim n_c^{1/2}$, indicating a fundamental trade-off between information and response time in the system: higher precision and faster response time favor larger and smaller n_c, respectively. Fig. 3(c) shows a heat map of the mutual information as a function of both θ and h. In addition to again seeing that I is maximal at $\theta = 0$, we also see that moving away from $h = 0$ causes $I(\theta, h)$ to sharply decrease. The case $h \neq 0$ biases the baseline production rate, which dampens correlated fluctuations between the two cells and leads to loss of information.

What happens to the information when we relax the requirement for the two cells to be identical? Are there regimes with dissimilar cells that can communicate effectively? Letting $\theta_X \neq \theta_Y$, with $h_X = h_Y = 0$, we show in
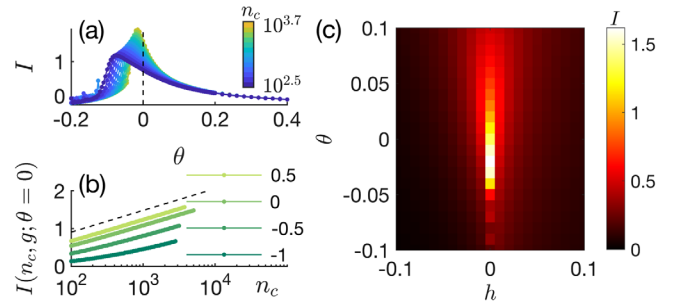
Fig. 4(a) that I is maximized in a narrow band which crosses $\theta_X = \theta_Y = 0$, with I decaying abruptly when $\theta_{X,Y} < 0$, but can remain appreciable when $\theta_{X,Y} > 0$. This is interesting, because Ising intuition normally proceeds that $T > T_c$ (read $\theta > 0$) is disordered and $T < T_c$ is ordered, but here the disordered pair holds higher mutual information farther away from the critical point. The abrupt decay at $\theta < 0$ is due to the polarized, bimodal distribution which makes it hard to communicate between the modes. When one cell is polarized ($\theta < 0$) and the other is centralized ($\theta > 0$), evidently the centralized cell mitigates
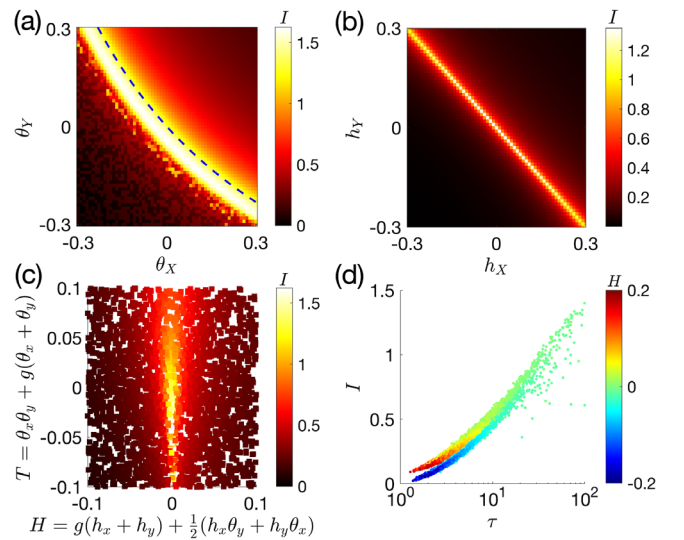

FIG. 4. Shannon mutual information for dissimilar cells. (a) Dissimilar θ values with $h_X = h_Y = 0$; blue dashes correspond to $T = 0$ from Eq. (4). (b) Dissimilar h values with $\theta_X = \theta_Y = 0$. (c) The mutual information I vs H, T (4), generated from randomly uniformly drawn $h_x, h_y, \theta_x, \theta_y \in [-0.1, 0.1]$. (d) Mutual information as a function of the correlation time τ for the data shown in c. In all plots, $g = 1$ and $k_1^- = q_1^- = 1$ with $n_c = 3000$.

the polarization when they are correctly matched, resulting in a high information manifold.

When we let $h_X \neq h_Y$ with $\theta_X = \theta_Y = 0$, the mutual information can remain high when $h_X + h_Y \approx 0$, shown in Fig. 4(b), in contrast to the symmetric $h_X = h_Y \neq 0$ case in Fig. 3(c). The case $h_X + h_Y \approx 0$ models a producer-consumer pair because the field h controls baseline production [3]. The pair, if rates are matched, shares information effectively. This is a second special limit of a high information manifold, which we detail in general below. Due to the universal nature of the dynamics near the bifurcation point, both the polarized-centralized pair and the producer-consumer pair show high information in other realizations of the dynamics, such as with Hill-function feedback (Fig. S1 of the Supplemental Material [16]). Thus, our simple model captures ubiquitous biological scenarios, showing they support high mutual information. Analytic results at the Gaussian limit [19] support this observation [16].

Having shown that a polarized-centralized pair and a producer-consumer pair can have high mutual information, two important questions arise: (i) can we explain the high-information manifolds observed in Figs. 4(a) and 4(b) theoretically? (ii) Do these high-information pairings depend on fine-tuning, $h_X = h_Y = 0$ for the polarized-centralized pair, and $\theta_X = \theta_Y = 0$ for the producer-consumer pair, or are there more realistic high-information pairings that do not depend on setting one pair of cellular parameters to zero? To answer these questions, we first define a set of two-cell collective coordinates.

Linearizing the deterministic steady state of the Landau form [Eq. (3)], we derive the collective coordinates (detailed in the Supplemental Material [16]),

$$T = \theta_X \theta_Y + g(\theta_X + \theta_Y),$$
$$H_X = g(h_X + h_Y) + h_X \theta_Y,$$
$$H_Y = g(h_X + h_Y) + h_Y \theta_X. \tag{4}$$

We further define a symmetric collective field, $H = \frac{1}{2}(H_X + H_Y)$. Note that $H_X = H_Y = 0$ is fulfilled when $\theta_X = \theta_Y = 0$ and $h_X + h_Y = 0$ as in Fig. 4(b). The case $h_X = h_Y = 0$ with $T = 0$ is shown in dashed blue in Fig. 4(a), consistent with the high I contour. The dependence of the mean molecule number as a function of H, T is shown in the Supplemental Material [16], Fig. S2, revealing the characteristic Ising state curves, but here for a two-cell collective state.

To test that the manifold given by $T = H = 0$ in Eq. (4) maintains high information in general, we uniformly draw random configurations of $h_X, h_Y, \theta_X, \theta_Y \in [-0.1, 0.1]$ and plot them on the H, T axes, colored by the mutual information, shown in Fig. 4(c). We see a peak at $T = H = 0$, confirming our expectation that this manifold implies high mutual information. Thus we extend the

simple high mutual information cases, shown in Figs. 4(a) and 4(b) to arbitrary values of h_X, h_Y, θ_X, θ_Y, ruling out fine-tuning to the critical point as a requirement.

By avoiding the critical point, the cells obtain high I near $T = H = 0$ but with $\theta_{X,Y}, h_{X,Y} \neq 0$. Do they also avoid critical slowing down? We return to the randomly drawn samples and plot I vs τ in Fig. 4(d). Interestingly, we note that all values of I for a set of $\{h_X, h_Y, \theta_X, \theta_Y\}$ collapse on two close branches uniquely determined by the correlation time τ. The branches are distinguished by the sign of H, with the lower branch corresponding to $H < 0$; this is expected since negative H lowers the mean molecule number, and having fewer molecules to exchange yields less information. The collapse shows that the time and information trade-off is strictly imposed: there is no "free lunch" where the cells can increase I without slowing down. The fact that the mutual information is uniquely defined by τ is a useful outcome since the correlation time is more readily observed empirically, in contrast to I which requires estimating a joint distribution function.

Discussion.—We have shown that coupling two idealized cells can give rise to a critical system. Extending the Schögl model, and capitalizing on a mapping between the internal dynamics of each cell and the mean-field Ising model, we cast each constituent of the system in terms of Ising-like quantities. At the collective bifurcation point, $\theta = h = 0$, mutual information is maximized, though dynamics are faced with a time and information trade-off due to critical slowing down. Further, a polarized-centralized pair or a producer-consumer pair support high mutual information away from the critical point. We generalize this observation and define a manifold of high mutual information states. However, being away from the critical point does not provide a way to increase information without increasing the correlation time of the system. Rather, the correlation time can serve as a proxy for mutual information in our system.

The mutual information between two cells, or their correlation time, can be directly measured from experimental data, such as fluorescence microscopy movies. As such, it is well-suited for high-throughput studies that quantify cellular dynamics from large-scale biological datasets. Here, we suggest a minimal model of cell-to-cell communication and, with it, a simple theoretical framework. Drawing on the universality of the dynamics near a critical point, the framework does not depend on a particular set of biochemical reactions, though in this manuscript we focused on an extension of Schögl's second model. The framework we present could be applied to translate experimental data to thermodynamic and information-theoretic quantities which are informative and interpretable.

---

*amugler@purdue.edu

[1] R. M. Vogel, A. Erez, and G. Altan-Bonnet, Nat. Commun. **7**, 12428 (2016).

[2] M. A. Muñoz, Rev. Mod. Phys. **90**, 031001 (2018).

[3] A. Erez, T. A. Byrd, R. M. Vogel, G. Altan-Bonnet, and A. Mugler, Phys. Rev. E **99**, 022422 (2019).

[4] I. Bose and S. Ghosh, J. Stat. Mech. (2019) 043403.

[5] T. A. Byrd, A. Erez, R. M. Vogel, C. Peterson, M. Vennettilli, G. Altan-Bonnet, and A. Mugler, Phys. Rev. E **100**, 022415 (2019).

[6] J. B. Huppa and M. M. Davis, Nat. Rev. Immunol. **3**, 973 (2003).

[7] H. Daneshpour and H. Youk, Curr. Opin. Syst. Biol. **18**, 44 (2019).

[8] F. Schlögl, Z. Phys. **253**, 147 (1972).

[9] P. Grassberger, Z. Phys. B **47**, 365 (1982).

[10] G. Dewel, D. Walgraef, and P. Borckmans, Z. Phys. B **28**, 235 (1977).

[11] G. Nicolis and M. Malek-Mansour, J. Stat. Phys. **22**, 495 (1980).

[12] M. Brachet and E. Tirapegui, Phys. Lett. **81A**, 211 (1981).

[13] S. Prakash and G. Nicolis, J. Stat. Phys. **86**, 1289 (1997).

[14] D.-J. Liu, X. Guo, and J. W. Evans, Phys. Rev. Lett. **98**, 050601 (2007).

[15] M. Vellela and H. Qian, J. R. Soc. Interface **6**, 925 (2009).

[16] See the Supplemental Material at http://link.aps.org/supplemental/10.1103/PhysRevLett.125.048103 for additional derivations, two figures, and data and code availability.

[17] M. B. Thompson, arXiv:1011.0175.

[18] N. G. Van Kampen, *Stochastic Processes in Physics and Chemistry* (Elsevier, New York, 1992), Vol. 1.

[19] F. C. Klebaner, *Introduction to Stochastic Calculus with Applications* (World Scientific, Singapore, 2012).